Computational evaluation of ScB and TiB MBenes as promising anode materials for high-performance metal-ion batteries

Yameng Li, Tao Zhao, Lei Li, Rao Huang, and Yuhua Wen*
Department of Physics, Xiamen University, Xiamen 361005, China

(Received 20 November 2021; accepted 5 April 2022; published 26 April 2022)

Emerging as a new family of two-dimensional materials, transition-metal borides, namely MBenes, are expected to possess outstanding physical and chemical properties owing to their layered structures analogous to MXenes. Here, we explore the electrochemical properties of ScB and TiB monolayers as anode materials for lithium- and sodium-ion batteries by density-functional theory calculations. Our results reveal that Li/Na ions can be stably adsorbed on surfaces of both monolayers with moderate adsorption energy, rapid charge/discharge rate, higher storage capacity, and much lower diffusion energy barrier (0.108 eV for Li ion on ScB, 0.105 eV for Li ion on TiB, 0.072 eV for Na ion on ScB, and 0.063 eV for Na ion on TiB) as compared with other MBene monolayers currently reported. Meanwhile, the open-circuit voltages all fall in the range of 0–1 V for Li/Na ion on the monolayers, which may effectively suppress the formation of Li/Na dendrite on anodes during the charge/discharge process. Besides, at room temperature, Li adatoms could be adsorbed on the monolayers more stably than Na adatoms. Our work demonstrates that ScB and TiB monolayers should be promising two-dimensional anode materials for lithium-ion batteries and are less suitable for sodium-ion batteries. These results advance our understanding on the electrochemical performances of MBenes and provide important insights into the design and development of high-performance electrode materials for metal-ion batteries.

DOI: 10.1103/PhysRevMaterials.6.045801

I. INTRODUCTION

With accelerating exploration of the next-generation battery technologies over the past years, developing the electrode materials with high electrical conductivity, large ion diffusion channels and abundant active sites have been a key issue in efficient energy storage and conversion devices [1–3]. Since the discovery of graphene in 2004, more and more emerging two-dimensional (2D) materials have been investigated as potential candidates for electrode materials in lithium- and sodium-ion batteries (LIBs and SIBs, respectively) [3,4]. As newly emerging 2D versatile materials, the transition-metal nitrides/carbides/carbonitrides (named MXenes) have attracted ever-increasing interest from both theoreticians and experimentalists after their successful syntheses [5–7]. Importantly, they have exhibited broad application prospects in energy storage and conversion and catalytic reactions owing to their intriguing structures and tunable electronic, optical, and electrochemical properties [6–8]. For example, the transition-metal core layers in MXenes could facilitate rapid electron transport through the electrode and thus enable charge storage at ultrahigh rates, while their transition-metal-oxidelike surfaces are capable of providing redox-active sites for pseudocapacitive charge storage [7]. Furthermore, the combination of these two structures and their large and tunable interlayer spaces, excellent hydrophilicity, extraordinary conductivity, compositional diversity, and abundant surface chemistries endow them with promising prospects as electrode materials for metal-ion batteries (MIBs) [7–11].

Recently, transition-metal borides (MBenes), as the new family of MXene derivatives, have also been attracting growing attention as electrode materials for the next-generation rechargeable MIBs. Similar to the synthesis of MXenes, the MBenes could be acquired through a multistep topochemical method by gradually exfoliating A atomic layers from MAB phases (ternary layered transition-metal borides, where M represents transition metal, A represents aluminum or indium, and B represents boron), leaving loosely stacked MB layers behind [12–15]. As newly emerging 2D materials analogous to MXenes, the MBenes with metallic surfaces and large specific surface areas also exhibit competitive electrochemical properties [16–21]. More importantly, they have been demonstrated to exhibit superior catalytic activity for nitrogen reduction reaction and hydrogen evolution reaction, and also emerge highly desirable for applications in LIBs and SIBs [17–22]. Among currently reported MBenes, MoB, and FeB monolayers have been theoretically verified to possess an omnidirectional small diffusion energy barrier and high storage capacity for Li atom [21], and VB, CrB, and MnB monolayers have been demonstrated to have high Young's modulus and unique in-plane anisotropy, low diffusion potential, and low open-circuit voltage as anode materials for LIBs and SIBs [22]. By inspiration of the fact that lightweight pristine MXenes, such as Sc_2C and Ti_2C MXene monolayers, present better electrochemical performance as electrode materials than pristine V_2C, Mo_2C, Zr_2C, Nb_2C, and Cr_2C MXene monolayers [23–29], it is expectable that pristine ScB and TiB MBene monolayers, applied as anode materials for LIBs

*yhwen@xmu.edu.cn

or/and SIBs, could also display electrochemical performances superior to previously reported VB, CrB, MoB, FeB, and MnB MBene monolayers. However, to the best of our knowledge, the relevant investigation is still lacking nowadays.

Herein, in this work, we report the electrochemical performances of ScB and TiB monolayers as anode materials for LIBs/SIBs by using first-principles calculations. The dynamical stability of both monolayers was verified by the phonon dispersion calculations and *ab initio* molecular dynamics (AIMD) simulations. According to the adsorption characteristics of single Li/Na ion on the monolayers, we further evaluated their electrochemical properties from many aspects including diffusion energy barrier of Li/Na ion, diffusion constants, open-circuit voltages (OCVs), storage capacity, and adsorption stability. In consideration of the lowest diffusion energy of Li/Na ion on VB monolayer among the reported MBenes, the electrochemical performances of VB monolayer as anode material for LIBs/SIBs were also examined for comparison with ScB and TiB monolayers. With the aim of exploring potential candidate as anode materials, our work is of significance for fundamentally understanding the electrochemical properties of pristine 2D materials and further development of high-performance electrode materials.

II. COMPUTATIONAL DETAILS

All theoretical calculations were within the framework of density-functional theory (DFT) in which the electron-ion interactions were described by the projector augmented wave potentials, as implemented in the Vienna *Ab initio* Simulation Package (VASP) [30,31]. The generalized gradient approximation of Perdew-Burke-Ernzerhof functional was performed to compute the exchange-correlation energy [32]. The plane waves used for expanding the Kohn-Sham electron wave functions have an energy cutoff of 500 eV [33]. For van der Waals interactions, the DFT-D3 scheme of dispersion correction was selected to correct the interaction between adsorbates and monolayers [34]. In order to avoid the virtual interactions in periodic boundary conditions, a large vacuum space of 20 Å was constructed along the Z-axis direction. During the structural optimization, the Monkhorst-Pack meshes were set to contain $5\times5\times1$ k point for $3\times3\times1$ supercell and $15\times15\times1$ for unit cell in Brillouin zones [35]. All geometric structures were fully relaxed until the convergence tolerances of total energy and Hellmann-Feynman force were smaller than 1×10^{-6} eV/atom and 0.01 eV/Å, respectively. Additionally, the density-function perturbation (DFPT) method as implemented in PHONOPY code was used to examine the dynamical stability of relaxed structure, followed by further confirmation through AIMD simulations for 20 ps within the canonical ensemble (NVT) at 300 K. [20–22,29,36,37] To explore the diffusion pathways and the corresponding energy barriers of Li/Na ion on ScB, TiB, and VB monolayers, we adopted the climbing image nudged elastic band (CI-NEB) method in the DFT calculations [38]. Meanwhile, the phonon frequencies of initial, transition, and final states were calculated over $\mathbf{\Gamma}$ points by DFPT method to notarize the minimum-energy pathway of Li/Na ion, and the Wigner corrections of the classical barrier were used to obtain the diffusion coefficients at different temperatures [39,40]. In addition, it should be noted

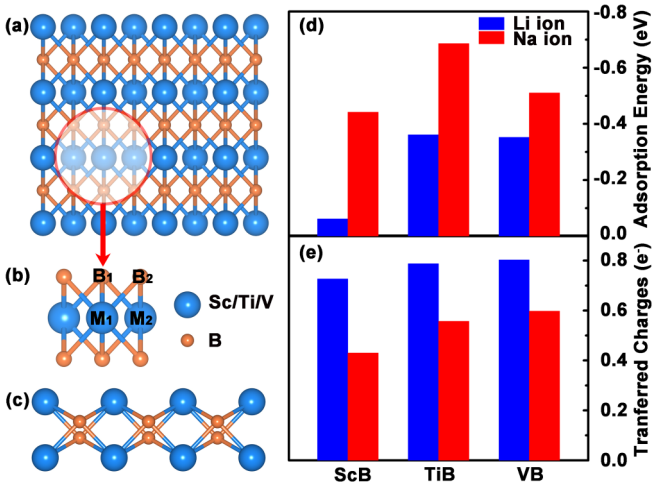

FIG. 1. (a) Top and (c) side views of optimized ScB monolayer, and (b) four high-symmetrical sites (M_1-, M_2-, B_1-, B_2 site). (d) The adsorption energy and (e) transferred charges of single Li and Na ions on the favorable adsorption sites of ScB, TiB, and VB monolayers.

that restricted by the scope and capacity of the DFT-based calculations, the solid-liquid interactions between the anode and its surrounding solvent/electrolyte environment were not considered. Therefore, the obtained results from pristine MBene monolayers may deviate from the related experimental results to a different extent.

III. RESULTS AND DISCUSSION

Firstly, we investigated the structure and electronic properties of ScB, TiB, and VB monolayers. Taking ScB monolayer as an example, it is composed of two outmost Sc layers and one intermediates zigzag diatomic B layer, and belongs to the orthorhombic space group *Cmcm* (No. 63), as illustrated in Figs. 1(a) and 1(c). After full relaxation, the lattice constants are $a = 3.109$ (ScB), 2.964 (TiB), and 2.918 (VB) Å, $b =$ 3.341 (ScB), 3.178 (TiB), and 3.223 (VB) Å. Other structural features were presented in our previous work [18]. To further examine the dynamical stability of the three MBenes, we performed the phonon dispersion calculations with the DFPT method and the AIMD simulations for 20 ps at 300 K. One can see from Fig. S1 in the Supplemental Material (SM) [41] that no imaginary frequency can be observed in the Brillouin zones of ScB, TiB, and VB monolayers, implying that they are structurally stable. Moreover, all the monolayers have no bond rupture or reconstruction after the relaxation, and the total energy slightly fluctuates within a small range (see Fig. S1 in the SM [41]) suggesting that they are thermodynamically stable at room temperature. Besides, the electronic structures of ScB, TiB, and VB monolayers display a distinct metallic characteristic with abundant electronic states at the Fermi level [see Figs. S2(a)–S2(c) in the SM [41]], which is mainly attributed to the metal atoms in these monolayers. Specially, this metallic feature provides an intrinsic advantage for all the monolayers as anode materials for LIBs and SIBs.

As depicted in Fig. 1(b), there are four preferential high-symmetrical sites on surfaces of ScB, TiB, and VB

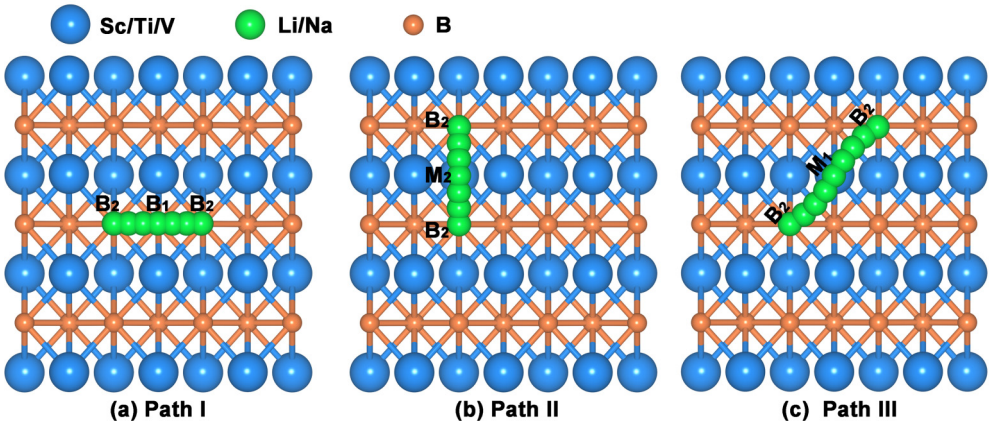

FIG. 2. Three preferential diffusion pathways of Li/Na ions between two adjacent B_2 sites on MB monolayer: (a) $B_2 \rightarrow B_1 \rightarrow B_2$, (b) $B_2 \rightarrow M_2 \rightarrow B_2$, and (c) $B_2 \rightarrow M_1 \rightarrow B_2$.

monolayers, labeled as M_1-, M_2-, B_1-, and B_2 sites, respectively. The feasibility of single Li/Na ion adsorbed on these sites was firstly examined. The corresponding adsorption energy was calculated by the following equation:

$$E_{ad} = \left(E_{\mathrm{MB}+n\mathrm{Li/Na}} - E_{\mathrm{MB}} - nE_{\mathrm{Li/Na}}\right)/n, \qquad (1)$$

where $E_{\mathrm{MB}+n\mathrm{Li/Na}}$ and E_{MB} are the total energy with and without Li/Na ion adsorption on MB (ScB, TiB, or VB) monolayer, respectively; $E_{\mathrm{Li/Na}}$ is the energy of per Li atom in bulk, and n is the number of adsorbed Li/Na ions. After full relaxation, Li ion can be stably adsorbed on B_2 site of ScB and VB monolayers, M_1- and B_2 sites of TiB monolayer. Meanwhile, the stable adsorption sites for Na ions are M_1-, M_2-, and B_2 sites of ScB monolayer, M_1- and B_2 site of TiB monolayer, and M_1-, B_1-, and B_2 sites of VB monolayer. The corresponding adsorption energies are summarized in Table S1 in the SM [41]. Evidently, the most favorable adsorption site was ascertained to be B_2 site for Li/Na ion on all the monolayers, and the corresponding adsorption energy is –0.062, –0.361, and –0.352 eV for Li ion and –0.442, –0.686, and –0.510 eV for Na ion on ScB, TiB, and VB monolayer, respectively, as shown in Fig. 1(d). Except for Li ion on ScB monolayer, the strong interactions between Li/Na ion and MB monolayer are beneficial to impeding the aggregation of individual Li/Na atoms. By comparison of these energies, the adsorption strength of Na ion is much stronger than that of Li ion on each monolayer. Moreover, the adsorption strengths of Li and Na both follow the order of TiB > VB > ScB. In comparison with the results of MXenes (–0.31, –0.721, and –0.96 eV for Li ion, and –0.61, –0.79, and –1.16 eV for Na ion on surfaces of pristine Sc_2C, Ti_2C, V_2C monolayers, respectively) [23,25,42,43], the MXenes exhibit markedly stronger adsorption strength for both Li and Na ions than the MBenes. Moreover, the stronger adsorption strength of Na ion than Li ion also occurs on the MXenes. In order to further shed light on the adsorption mechanism, the Bader charges analysis was used to examine the adsorption of single Li/Na ion on ScB, TiB, and VB monolayers. The charges transferred from single Li or Na ion into the surface of MB monolayer are illustrated in Fig. 1(e). One can find that the transferred charges are considerable, and the amount of transferred charges from Li ion is larger than that from Na ion. Specifically, the transferred charges are contributed from four metal atoms and the neighboring three borides. Moreover, the trend of charge transfer, i.e., the order of VB > TiB > ScB for Li/Na ion, is different from that of the adsorption energy [see Figs. 1(d) and 1(e)], which could be ascribed to the number of valence electrons per metal atom. Therefore, the charge transfer and the adsorption energy jointly suggest that ScB monolayer is weaker for the adsorption of Li/Na ion than both TiB and VB monolayers.

The charge/discharge rate is an important factor for assessing the electrochemical performances of electrode materials. Based on the aforementioned results, we further investigated the charge/discharge rates by the diffusion kinetics of Li/Na ions between two adjacent B_2 sites, which are the most favorable adsorption sites. We chose three preferential diffusion pathways on two adjacent B_2 sites (see Fig. 2), i.e., $B_2 \rightarrow B_1 \rightarrow B_2$ (path I), $B_2 \rightarrow M_2 \rightarrow B_2$ (path II), and $B_2 \rightarrow M_1 \rightarrow B_2$ (path III), and calculated their corresponding energy barriers by using the CI-NEB method. As illustrated in Fig. 3, for all the surfaces, path I is the most favorable. Specifically, the lowest diffusion energy barriers on ScB, TiB, and VB monolayers are 0.108 and 0.105, and 0.264 eV for Li ion, and 0.072, 0.063, and 0.085 eV for Na ion, respectively. Evidently, the diffusion energy barrier of Na ion is lower than that of Li ion on the same monolayer, implying the higher migration rate of Na ion than Li ion. For path III, the diffusion energy barrier of Li/Na ion is about twice that of path I, suggesting that Li and Na ions are difficult to migrate from B_2 to M_2 and to B_2 site. Comparing the migration characteristics of Li and Na ions on these monolayers, one can see that the diffusion energy barriers of metal (Li or Na) ion on ScB and TiB monolayers are lower than that on VB monolayers, indicating that the charge/discharge rates on the former should be higher than that on the latter. In comparison with the diffusion barriers of MXenes (0.018, 0.016, and 0.025 eV for Li ion, and 0.012, 0.021, and 0.016 eV for Na ion on pristine Sc_2C, Ti_2C, and V_2C monolayers, respectively) [23,25,42,43], ScB and TiB monolayers exhibit much higher barriers than the MXenes, implying the slower charge/discharge rates for Li/Na ion on the former than the latter. However, both ScB and TiB monolayers should possess faster charge/discharge rates for Li/Na ion than other MBenes, such as CrB (the diffusion

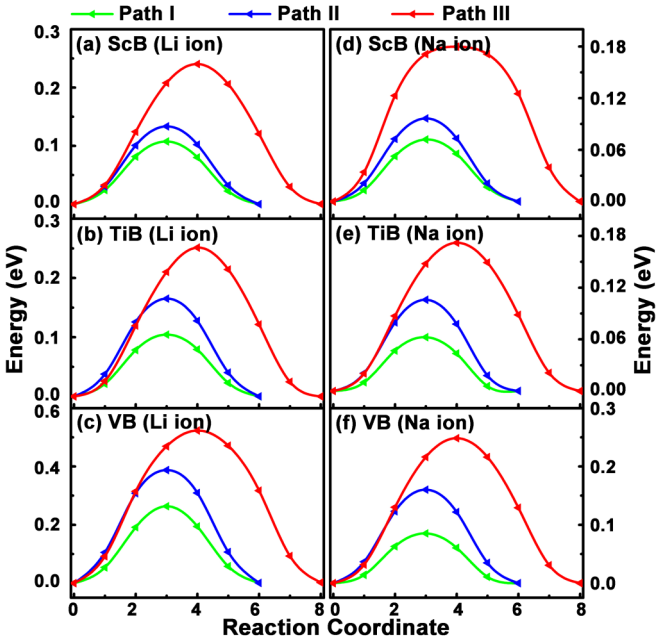

FIG. 3. The diffusion energy barriers of Li ion on (a) ScB, (b) TiB, and (c) VB monolayers, and of Na ion on (d) ScB, (e) TiB, and (f) VB monolayers.

energy barrier of 0.28 eV), MoB (0.27 eV), FeB (0.24 eV), and MnB (0.29 eV) for Li ion, CrB (0.17 eV), and MnB (0.17 eV) for Na ion [21,22]. Therefore, these two MBenes should both be superior electrode materials for LIBs and SIBs to other MBenes while inferior to the aforementioned MXenes.

To further explore the diffusive behaviors of Li/Na ion on ScB and TiB monolayers, we examined the quantum diffusion rate by incorporating the quantum effects into the classical barriers [39,40]. The corresponding results of the Wigner zero-point energy (ZPE)-tunneling corrected diffusion constant are listed in Table I, in which the classical diffusion constants are also provided for comparison. Evidently, one can see that the quantum effects on the diffusion of Li ion on TiB monolayer are much smaller than on ScB monolayers, whereas the opposite situation occurs in the quantum effects of Na ion diffusion on the two monolayers. Furthermore, the temperature has a great influence on whether the quantum effects are considered or not. Specially, the two diffusion constants are, respectively, up to 4.792×10^{7} and 4.959×10^{7} s^{-1} for Li ion on ScB monolayer at 300 K, which are slightly higher than the values on TiB monolayers. However, the situation is the opposite at 100 K, indicating that the effect of temperature on diffusion is more remarkable on ScB monolayer. Note that the two diffusion constants of Li ion on two MBene monolayers are significantly higher than on other 2D materials, including h-BN/Pn heterostructure, SiS, SiSe, Ti_2CT_2, V_2CT_2, and $TiVCT_2$ (T = O, F, or S) monolayers, but slightly lower than on pristine Ti_2C, V_2C, and TiVC monolayers [39,40,42]. As for the migration of Na ion at 300 K, the two diffusion constants of 1.691×10^{11} and 1.760×10^{11} s^{-1} on ScB monolayer and of 2.122×10^{11} and 2.230×10^{11} s^{-1} on TiB monolayer are markedly higher than those of Li ion on the same monolayers, in agreement with the analyses of diffusion energy barrier. Besides, the quantum mechanical tunneling (QMT) enhanced the diffusion of Li and Na ions on these monolayers at different temperatures, as indicated by Table I.

In order to further explore the electrochemical performances of MB monolayers as electrode materials for LIBs and SIBs, we introduced the OCV as a function of storage capacity (C_M) of Li/Na ions on ScB, TiB, and VB monolayers. The OCV is widely used to evaluate the electrochemical properties of electrode materials. Specifically, the OCV and C_M can be obtained by the following equations:

$$\mathrm{OCV} \approx \frac{E_{\mathrm{MB}} + nE_{\mathrm{Li/Na}} - E_{\mathrm{MB}+n\mathrm{Li/Na}}}{nzF}, \tag{2}$$

$$C_{\mathrm{M}} = \frac{nF}{M_{\mathrm{MB}} + nM_{\mathrm{Li/Na}}}, \tag{3}$$

where n, E_{MB}, $E_{\mathrm{Li/Na}}$, and $E_{\mathrm{MB}+n\mathrm{Li/Na}}$ are defined in Eq. (1), M_{MB} and $M_{\mathrm{Li/Na}}$ are the molar weights of MB monolayer and Li/Na atom, respectively; z is the electronic charges of Li/Na ion in the electrolyte ($z = 1$), and F is the Faraday constant (26 801 mAh/mol). Based on the aforementioned analyses of single Li/Na ion adsorbed on three monolayers, we examined the adsorption performance of multi-Li/Na ions at the most favorable adsorption site on the outmost layer of ScB, TiB, and VB monolayers. With the increasing concentration of adsorbed Li/Na ions, the OCVs for Li ions on ScB, TiB, and VB monolayers present a monotonous increase, whereas the OCVs for Na ions on these monolayers fluctuate slightly, as shown in Figs. 4(a) and 4(b). Especially, all the OCVs fall in the range of 0–1 V with increasing concentration of Li/Na ions on the three monolayers, which may effectively suppress the dendrite formation of Li/Na metals during the

TABLE I. The classical diffusion constant (K), with and without Wigner ZPE-tunneling corrected diffusion constants ($K_{\mathrm{Wig/tunn}}$) of Li/Na ion on ScB and TiB monolayers at three temperatures and their increasing percentage induced by QMT.

		Diffusion constant of Li ion			Diffusion constant of Na ion		
MBene	T	K(s^{-1})	$K_{\mathrm{Wig/tunn}}$(s^{-1})	QMT (%)	K(s^{-1})	$K_{\mathrm{Wig/tunn}}$(s^{-1})	QMT (%)
ScB	100	1.162×10^{7}	1.453×10^{7}	20.378	6.441×10^{8}	8.371×10^{8}	23.056
	200	5.981×10^{9}	6.424×10^{9}	6.896	4.200×10^{10}	4.568×10^{10}	8.056
	300	4.792×10^{10}	4.959×10^{10}	3.368	1.691×10^{11}	1.760×10^{11}	3.920
TiB	100	1.392×10^{7}	1.489×10^{7}	6.514	1.686×10^{9}	2.248×10^{9}	25.000
	200	5.983×10^{9}	6.160×10^{9}	2.873	6.336×10^{10}	6.996×10^{10}	9.434
	300	4.516×10^{10}	4.586×10^{10}	1.526	2.122×10^{11}	2.230×10^{11}	4.843

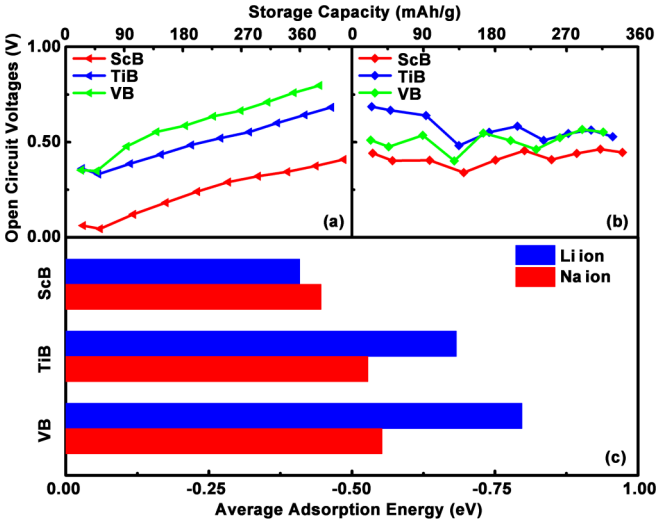

FIG. 4. The open-circuit voltage as a function of storage capacity of (a) Li ion and (b) Na ion on ScB, TiB, and VB monolayers. (c) The average adsorption energy of multi-Li/Na ions on the most favorable adsorption site on these monolayers.

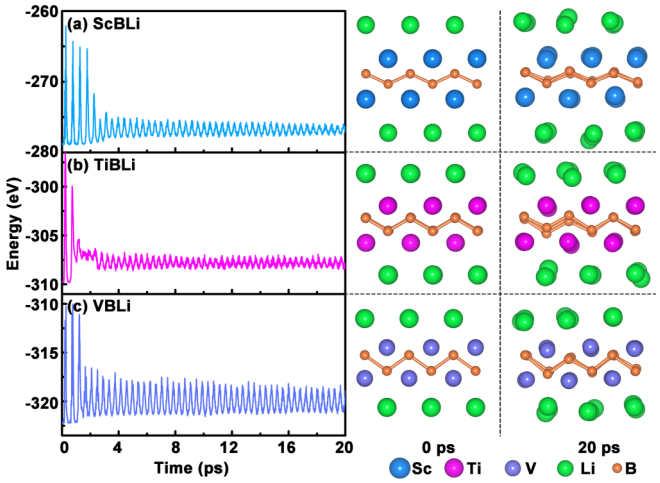

FIG. 5. The energy evolutions of Li ion absorbed (a) ScB, (b) TiB, and (c) VB monolayers during AIMD simulations of 20 ps at 300 K. The corresponding structures at 0 and 20 ps are shown in the right panel.

charge/discharge process [22,42]. When the upper and lower surfaces of each monolayer are fully covered with Li/Na ions, the OCVs on ScB, TiB, and VB monolayers, respectively, reach 0.409, 0.683, and 0.797 V for Li ion, and 0.446, 0.528, and 0.553 V for Na ion. Evidently, the OCVs follow the order of ScB < TiB < VB for Li and Na ions. By comparison with pristine MXenes, the OCV values of Li/Na ion on ScB monolayer are a bit larger than those on Sc_2C monolayer (0.32 V Li ion and 0.23 V for Na ion), while smaller than those on Sc_2N monolayer (0.48 V for Li ion) [23,44]. In contrast, the OCV values of Li/Na ions on TiB and VB monolayers are remarkably lower than those on Ti_2N monolayer (1.345 V for Li ion and 0.882 V for Na ion) and V_2C monolayer (0.82 V for Li ion and 0.56 V for Na ion) [25,45]. The storage capacities of Li/Na ion on ScB and TiB monolayers, i.e., 427.373 and 408.421 mAh/g for Li ion, and 340.287 and 328.162 mAh/g for Na ion, follow the order of ScB > TiB > VB. Although their values are smaller than those of Sc_2N, Ti_2N, Sc_2C, and V_2C monolayers to different extents [23,25,43,44], they are higher as compared with VB monolayers (390.168 mAh/g for Li ion and 316.273 mAh/g for Na ion) and graphite (372 mAh/g for Li ion). Especially, compared to graphite, the advantages of ScB and TiB monolayers in the theoretical capacity may not be remarkable, but the diffusion energy barriers of Li ion for ScB and TiB monolayers (0.108 and 0.105 eV, respectively) are much lower than that of graphite (0.30 eV) [46], demonstrating that the former should be superior to the latter when they are considered as anode materials. These results further confirm the excellent electrochemical performances of ScB and TiB monolayers as anode materials for LIBs or SIBs.

Besides, the average adsorption energies of multi-Li/Na ions on ScB, TiB, and VB monolayers were calculated according to Eq. (1), as illustrated in Fig. 4(c). One can see that the adsorption strength of Li ion is much stronger than that of Na ion for absorbing on TiB and VB monolayers, whereas slightly weaker than that of Na ion for absorbing on ScB monolayer. To be specific, the average adsorption energies are –0.409, –0.683, and –0.797 eV for Li ions, and –0.446, –0.528, and –0.553 eV for Na ions on ScB, TiB, and VB monolayers, respectively. Evidently, the adsorption capability of Li ion follows the order of VB > TiB > ScB, while the opposite order occurs for Na ion. In addition, we also examined the interaction between Li/Na ions and substrates (i.e., pristine ScB, TiB, and VB monolayers) by calculating the projected density of states when both surfaces of each monolayer are fully covered with Li/Na ions. As presented in Figs. S2(d)–S2(i) of the SM [41], ScB, TiB, and VB monolayers still maintained the metallic characteristic after the adsorption of Li/Na ions, and the strong hybridized interactions between metal Sc/Ti/V and Li/Na atoms were observed. These results intuitively confirm the adsorption stability of Li/Na ions on these monolayers, indicating that ScB and TiB monolayers could be promising candidates as anode materials for LIBs/SIBs, superior to VB monolayer.

To inspect the adsorption stability of Li/Na ions, we also examined the thermostability of ScB, TiB, and VB monolayers fully covered with Li/Na ions through AIMD simulations within *NVT* ensemble. The total time of the simulations was set to be 20 ps, and the temperature was set at 300 K. As shown in Fig. 5, all Li adatoms kept thermodynamically stable at primitive adsorption sites on these monolayers after relaxation, and no significant reconstruction was observed. In addition, the total energies of ScBLi, TiBLi, and VBLi systems gradually converge within the relaxation time, further confirming the thermodynamic stability of these systems at room temperature. By comparison, the total energies converge more quickly in the ScBNa, TiBNa, and VBNa systems, and the fluctuations are also smaller (see Figs. S3(a)–3(c) in the SM [41]). Nonetheless, AIMD simulations at 300 K demonstrated that adsorbed Na ions cannot be anchored on the original sites. Some Na ions are separated from the surfaces (see Fig. S3 in the SM [41] for details), indicating that Na ions are partially unstable at room temperature. Especially,

the absence of Li/Na ion accumulation indicates that the formation of Li/Na dendrite may be effectively impeded during the charge/discharge process. From the perspective of AIMD results, the ScB and TiB monolayers are more suitable as anode materials for LIBs than for SIBs at room temperature.

IV. CONCLUSIONS

In summary, as emerging 2D materials, the electrochemical performances of ScB and TiB MBenes as anode materials for LIBs and SIBs were systematically investigated by using DFT calculations. Both the phonon dispersion calculation and AIMD simulation were employed to examine their structural and thermodynamical stability. Our calculations reveal that Li/Na ion can be stably adsorbed at B_2 sites on both monolayers with moderate adsorption energies. Li/Na ions tend to diffuse along the $B_2 \rightarrow B_1 \rightarrow B_2$ pathway with lower diffusion energy barrier of 0.108 and 0.105 eV for Li ion, and of 0.072 and 0.063 eV for Na ion on ScB and TiB monolayer as compared with VB monolayers (0.264 eV for Li ion and 0.085 eV for Na ion). The OCVs (storage capacity) can reach 0.409 (427.373 mAh/g) and 0.683 V (408.421 mAh/g) for Li ion, and 0.446 (340.287 mAh/g) and 0.528 V (328.162 mAh/g) for Na ion on ScB and TiB monolayers after full coverage of Li/Na ions, remarkably superior to the corresponding result on VB monolayer. The OCVs for Li/Na ion on the three monolayers all fall in the range of 0–1 V, which may effectively impede the formation of Li/Na dendrite during the charge/discharge process. More importantly, Li adatoms can be stably adsorbed on all the primitive adsorption sites of ScB and TiB monolayers at room temperature, whereas some of Na adatoms were separated from the surfaces of both monolayers, indicating that Li adatoms are adsorbed more stably than Na adatoms. Our results suggest that ScB and TiB monolayers should possess better electrochemical performances as anode materials for LIBs and SIBs as compared with other MBenes available (including VB monolayer), and exhibit more stable adsorption capability for Li ions than Na ions at room temperature. This work not only advances our understanding on the electrochemical properties of ScB and TiB MBenes but also provides important references for the design of high-performance electrode materials for MIBs.

ACKNOWLEDGMENTS

This work was financially supported by the National Natural Science Foundation of China (Grant No. 51871189 and No. 11474234). High Performance Computing Center of Xiamen University is acknowledged for the supercomputer resources.

[1] M. Winter, J. O. Besenhard, M. E. Spahr, and P. Novak, Adv. Mater. **10**, 725 (1998).
[2] J. M. Tarascon and M. Armand, Nature (London) **414**, 359 (2001).
[3] P. G. Bruce, B. Scrosati, and J. M. Tarascon, Angew. Chem. **120**, 2972 (2008).
[4] K. S. Novoselov, A. K. Geim, S. V. Morozov, D. Jiang, Y. Zhang, S. V. Dubonos, I. V. Grigorieva, and A. A. Firsov, Science **306**, 666 (2004).
[5] M. Naguib, M. Kurtoglu, V. Presser, J. Lu, J. Niu, M. Heon, L. Hultman, Y. Gogotsi, and M. W. Barsoum, Adv. Mater. **23**, 4248 (2011).
[6] M. Naguib, O. Mashtalir, J. Carle, V. Presser, J. Lu, L. Hultman, Y. Gogotsi, and M. W. Barsoum, ACS Nano **6**, 1322 (2012).
[7] A. VahidMohammadi, J. Rosen, and Y. Gogotsi, Science **372**, 1165 (2021).
[8] F. W. Ming, H. F. Liang, G. Huang, Z. Bayhan, and H. N. Alshareef, Adv. Mater. **33**, 2004039 (2021).
[9] M. R. Lukatskaya, O. Mashtalir, C. E. Ren, Y. Dall'Agnese, P. Rozier, P. L. Taberna, M. Naguib, P. Simon, M. W. Barsoum, and Y. Gogotsi, Science **341**, 1502 (2013).
[10] Q. Tang, Z. Zhou, and P. Shen, J. Am. Chem. Soc. **134**, 16909 (2012).
[11] N. Michael, H. Joseph, L. Jun, M. C. Kevin, H. Lars, G. Yury, and W. B. Michel, J. Am. Chem. Soc. **135**, 15966 (2013).
[12] L. T. Alameda, P. Moradifar, Z. P. Metzger, N. Alem, and R. E. Schaak, J. Am. Chem. Soc. **140**, 8833 (2018).
[13] H. M. Zhang, H. M. Xiang, F. Z. Dai, Z. L. Zhang, and Y. C. Zhou, J. Mater. Sci. Technol. **34**, 2022 (2018).
[14] L. T. Alameda, R. W. Lord, J. A. Barr, P. Moradifar, Z. P. Metzger, B. C. Steimle, C. F. Holder, N. Alem, S. B. Sinnott, and R. E. Schaak, J. Am. Chem. Soc. **141**, 10852 (2019).
[15] J. Wang, T. N.Ye, Y. Gong, J. Wu, N. Miao, T. Tada, and H. Hosono, Nat. Commun. **10**, 2284 (2019).
[16] Z. Jiang, P. Wang, X. Jiang, and J. J. Zhao, Nanoscale Horiz. **3**, 335 (2018).
[17] B. K. Zhang, J. Zhou, Z. L. Guo, Q. Peng, and Z. M. Sun, Appl. Surf. Sci. **500**, 144248 (2020).
[18] Y. M. Li, L. Li, R. Huang, and Y. H. Wen, Nanoscale **13**, 15002 (2021).
[19] S. Qi, Y. Fan, L. Zhao, W. Li, and M. Zhao, Appl. Surf. Sci. **536**, 147742 (2021).
[20] X. Yang, C. Shang, S. Zhou, and J. Zhao, Nanoscale Horiz. **5**, 1106 (2020).
[21] Z. Guo, J. Zhou, and Z. Sun, J. Mater. Chem. A **5**, 23530 (2017).
[22] J. Jia, B. J. Li, S. Q. Duan, Z. Cui, and H. T. Gao, Nanoscale **11**, 20307 (2019).
[23] X. Lv, W. Wei, Q. Sun, L. Yu, B. Huang, and Y. Dai, ChemPhysChem **18**, 1627 (2017).
[24] H. Zhang, Z. H. Fu, R. F. Zhang, Q. F. Zhang, H. Z. Tian, D. Legut, T. C. Germann, Y. Q. Guo, S. Y. Du, and J. S. Francisco, Proc. Natl. Acad. Sci. USA **114**, E11082 (2017).
[25] Y. M. Li, Y. L. Guo, and Z. Y. Jiao, Curr. Appl. Phys. **20**, 310 (2020).
[26] J. P. Hu, B. Xu, C. Y. Ouyang, Y. Zhang, and S. A. Yang, RSC Adv. **6**, 27467 (2016).
[27] J. Zhu, A. Chroneos, J. Eppinger, and U. Schwingenschlögl, Appl. Mater. Today **5**, 19 (2016).

[28] Z. Xu, X. Lv, J. Chen, L. Jiang, Y. Lai, and J. Li, Phys. Chem. Chem. Phys. **19**, 7807 (2017).
[29] Y. D. Yu, Z. L. Guo, Q. Peng, J. Zhou, and Z. M. Sun, J. Mater. Chem. A **7**, 12145 (2019).
[30] G. Kresse and J. Furthmüller, Phys. Rev. B **54**, 11169 (1996).
[31] G. Kresse and D. Joubert, Phys. Rev. B **59**, 1758 (1999).
[32] J. P. Perdew, K. Burke, and M. Ernzerhof, Phys. Rev. Lett. **77**, 3865 (1996).
[33] J. P. Perdew and Y. Wang, Phys. Rev. B **33**, 8800 (1986).
[34] S. Grimme, J. Antony, S. Ehrlich, and H. Krieg, J. Chem. Phys. **132**, 154104 (2010).
[35] H. J. Monkhorst and J. D. Pack, Phys. Rev. B **13**, 5188 (1976).
[36] A. Togo and I. Tanaka, Scr. Mater. **108**, 1 (2015).
[37] J. Hafner, J. Comput. Chem. **29**, 2044 (2008).
[38] G. Henkelman, J. Chem. Phys. **113**, 9901 (2000).
[39] C. Chowdhury, S. Karmakar, and A. Datta, ACS Energy Lett. **1**, 253 (2016).
[40] S. Karmakar, C. Chowdhury, and A. Datta, J. Phys. Chem. C **120**, 14522 (2016).
[41] See Supplemental Material at http://link.aps.org/supplemental/10.1103/PhysRevMaterials.6.045801 for full details on the results.
[42] Y. M. Li, L. Li, R. Huang, Y. Zhang, and Y. H. Wen, Nanoscale **13**, 2995 (2021).
[43] Y. Xiao, Y. Ding, H. Cheng, and Z. Lu, Comput. Mater. Sci. **163**, 267 (2019).
[44] A. Samad and U. Schwingenschlögl, Phys. Rev. Appl. **15**, 034025 (2021).
[45] D. Wang, Y. Gao, Y. Liu, D. Jin, Y. Gogotsi, X. Meng, F. Du, G. Chen, and Y. Wei, J. Phys. Chem. C **121**, 13025 (2017).
[46] K. Toyoura, Y. Koyama, A. Kuwabara, and I. Tanaka, J. Phys. Chem. C **114**, 2375 (2010).